

Ordering of Nitrogen in Nickel Nitride Ni₃N Determined by Neutron Diffraction

Andreas Leineweber,^{†,‡} Herbert Jacobs,^{*,†} and Steve Hull[§]

Lehrstuhl Anorganische Chemie, Fachbereich Chemie der Universität, 44221 Dortmund, Germany, and ISIS, Rutherford Appleton Laboratory, Chilton OX11, 0QX, U.K.

Received May 8, 2001

The metallic interstitial nitride Ni₃N was prepared from Ni(NH₃)₆Cl₂ and NaNH₂ in supercritical ammonia (*p*(NH₃) ≈ 2 kbar) at 523 K. Its previously reported crystal structure, as determined from X-ray powder data, was confirmed by neutron powder diffraction: Ni₃N crystallizes in the hexagonal ϵ -Fe₃N-type structure (*P*6₃22, *Z* = 2, *a* = 4.6224 Å and *c* = 4.3059 Å at room temperature). The N atoms on the octahedral sites of an *hcp* arrangement of Ni show virtually complete occupational order at ambient temperatures, which is preserved up to its thermal decomposition at *T* ≈ 600 K. This behavior is in marked contrast to that of the isotopic iron nitride, ϵ -Fe₃N, which shows reversible partial disordering within the same range of temperatures. Possible reasons for the different behaviors of the two nitrides ϵ -Fe₃N and Ni₃N are discussed.

Introduction

The first reported synthesis of Ni₃N used Ni powder and flowing ammonia at 450 °C.¹ Another route starts from Ni(NH₂)₂ (obtained from Ni²⁺ and NH₂⁻ in liquid ammonia), which decomposes under intermediate formation of a probably amorphous Ni₃N₂, finally giving Ni₃N at about 200 °C.^{2–4} Synthesis from Ni and N₂ has not yet been reported, and equilibrium pressures are expected to be very high.¹

As with most other binary nitrides of 3d metals, Ni₃N can be regarded as a metallic interstitial compound:⁵ these have an arrangement of metal atoms that is typical for a metal (mostly *fcc*, *hcp*, or *bcc*, not necessarily the same arrangement as for the pure metal) and N (or O, C, B, H) in interstices, in most cases on octahedral sites in a more or less ordered way. The metal–metal interactions are metal-like, and N is bonded covalently to the metal atoms. Bonding and electronic structure of interstitial nitrides are still a topic of many publications, also from a more or less chemical point of view.^{6,7}

The crystal structure of Ni₃N^{1,8} is based on an *hcp* arrangement of Ni in which N occupies octahedral sites, expanding the volume referring to nickel (the pure element is *fcc*) by 21%. The N atoms on the octahedral sites are ordered in such a way that the structure type of ϵ -Fe₃N⁹ results. This has the space group symmetry *P*6₃22 and unit cell dimensions increased by 3^{1/2} × 3^{1/2} × 1 relative to the *hcp* cell (Figure 1). The ordered

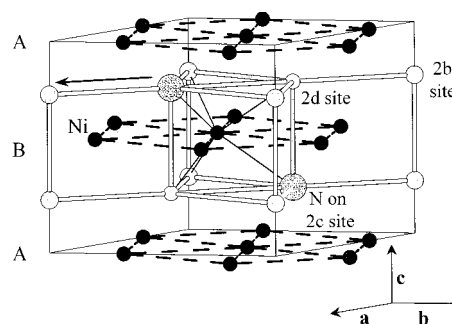


Figure 1. ϵ -Fe₃N-type structure of Ni₃N. Crystallographically different octahedral sites in *P*6₃22 are labeled. Site 2c is the main site for N, and 2b is the main disorder site. The arrow indicates the reversible partial positional disordering of N at elevated temperatures as observed for ϵ -Fe₃N. The thick lines connecting the octahedral sites do not represent bonds but serve for orientation. The edges of one trigonal prism formed by a set of six octahedral sites as shown in Figure 5 are highlighted in gray. Broken lines indicate close-packed layers of Ni with |AB|AB| stacking. Ni atoms in addition to those located within the indicated unit cell are shown to clarify their *hcp* arrangement.

distribution of N may be understood in terms of a minimization of repulsive N···N interactions. Only corner sharing of octahedra NNi₆ is present.

The ϵ -Fe₃N type or, for nonideal compositions and ordering of N, the “ ϵ -type” structures^{10,11} are quite common for binary nitrides of 3d metals.⁵ However, in contrast to other ϵ -type carbides, nitrides, and oxides, including nitrides of earlier 3d elements, Ni₃N is restricted to its stoichiometric composition. There is only one report¹² that gives a composition of Ni₃N_{1.16} for a hexagonal nickel nitride. However, its unit cell parameters are exactly those given elsewhere for the composition Ni₃N.^{1–3,8} For other M–N systems (M = V–Co),⁵ a considerable variation of unit cell parameters with composition is found. Therefore, it is probable that the composition Ni₃N_{1.16},¹² deduced from chemical analysis (no details given), is wrong.

* Corresponding author. E-mail: jacobs@pop.uni-dortmund.de.

[†] Fachbereich Chemie der Universität Dortmund.

[‡] Present address: Max-Planck-Institut für Metallforschung, Seestr. 92, 70174 Stuttgart, Germany.

[§] Rutherford Appleton Laboratory.

(1) Juza, R.; Sachsze, W. *Z. Anorg. Allg. Chem.* **1943**, *251*, 201.

(2) Watt, G. W.; Davies, D. D. *J. Am. Chem. Soc.* **1948**, *70*, 3753.

(3) Tenten, A.; Jacobs, H. *J. Less-Common Met.* **1991**, *170*, 145.

(4) Tenten, A. Ph.D. Thesis, Universität Dortmund, Dortmund, Germany, 1991.

(5) Juza, R. *Adv. Inorg. Chem. Radiochem.* **1967**, *9*, 81.

(6) Sifkovits, M.; Smolinski, H.; Hellwig, S.; Weber, W. *J. Magn. Magn. Mater.* **1999**, *204*, 191.

(7) Eck, B.; Dronskowski, R.; Takahashi, M.; Kikkawa, S. *J. Mater. Chem.* **1999**, *9*, 1527.

(8) Jack, K. H. *Acta Crystallogr.* **1950**, *3*, 392.

(9) Hendricks, S. B.; Kosting, P. B. *Z. Kristallogr.* **1930**, *74*, 511.

(10) Leineweber, A.; Jacobs, H. *J. Alloys Compd.* **2000**, *308*, 178.

(11) Leineweber, A. Ph.D. Thesis, Universität Dortmund, Dortmund, Germany, 1999.

(12) Arnott, R. J.; Wold, A. *J. Phys. Chem. Solids* **1960**, *15*, 152.

Nickel is the last element of the 3d metals that forms interstitial nitrides. On going from Ni to Cu, one finds that the character of the only known copper nitride, Cu₃N,¹³ changes: Cu₃N is a stoichiometric and semiconducting¹⁴ compound and, like Ni₃N, has octahedral coordination of N. Together with the Cu atoms, the relatively open-packed *anti*-ReO₃-type structure results.

In the work presented here, Ni₃N was regarded as a model system to compare it with results obtained on the isotypic ϵ -Fe₃N.¹⁵ For ϵ -Fe₃N at elevated temperatures, a reversible partial disordering of N on the octahedral sites was observed. By similar investigations on Ni₃N, the influence of the different metals on the ordering of N should result.

Experimental Section

Preparation, Chemical Analysis, X-ray Diffractometry, and Scanning Electron Microscopy. Severe problems in preparing large batches of Ni₃N by the reaction of Ni powder with flowing NH₃ are reported.¹ As a result, we chose a one-pot synthesis in supercritical ammonia including the formation of Ni(NH₂)₂ from Ni(NH₃)₆Cl₂ and NaNH₂ and its decomposition.

The starting material Ni(NH₃)₆Cl₂¹⁶ was prepared by passing NH₃ gas (99.999%, Messer-Griesheim, Frankfurt, Germany) into a saturated aqueous solution of NiCl₂·6H₂O (purity > 97%, Merck, Darmstadt, Germany) along with some NH₄Cl (>99.8%, Merck). The product crystallized from this solution upon slow cooling and was filtered. NaNH₂ was prepared from Na (99.5 wt %, Merck) reacted with an excess of liquid NH₃ in a steel autoclave at 100 °C.¹⁷

Ni(NH₃)₆Cl₂ (6–7 g) and NaNH₂ (molar ratio 1:2.05) were mixed together in a glovebox under dry argon and filled in a high-pressure autoclave (*V* = 15 mL).¹⁸ Especially sodium amide is very sensitive to moist air. The autoclave was filled with liquid NH₃ and heated to 100 °C within 3 h. Afterward, the temperature was increased to 250 °C by 30 °C/day, kept for 1 week at 250 °C (*p*(NH₃) ≈ 2 kbar), and cooled to ambient temperatures by switching off the furnace.

After the NH₃ was released, the autoclave was opened. The gray reaction product (mostly a mixture of NaCl and Ni₃N) was stirred in ethanol, filtered, and washed with an aqueous solution of NH₄Cl/NH₃ (each 0.5 M), with water, and afterward with ethanol and ether. The washing liquids contained small amounts of Ni²⁺ and some very fine powder particles that passed the funnel. The overall yield was typically 60–70%.

X-ray diffraction patterns (Guinier camera FR552, Enraf-Nonius, Delft, The Netherlands, CuKα₁ radiation) showed the reported hexagonal cell with *a* = 4.625(1) Å and *c* = 4.306(1) Å. According to the X-ray patterns, some batches of pure Ni₃N were synthesized. However, some batches contained small amounts of Ni or NiO. Pure batches had an analytical N content (combustion analysis performed on an Elemental Analyzer 1106, Erba, Mailand, Italy) of 7.4% (theoretical content: 7.37%; ≤0.1% C and H were present). There are no hints in the literature that a considerable fraction of N can be replaced by O in interstitial nitrides of “late” 3d metals of Mn–Ni, including Ni₃N.

For reasons of comparison, we reacted Ni(NH₃)₆Cl₂ with NaNH₂ in the absence of additional NH₃ in steel autoclaves¹⁹ with a similar temperature program. According to X-ray diffraction, the product contained Ni₃N with large amounts of Ni as an impurity. The reflections of both phases were very broad compared to those from the materials obtained in liquid resp. supercritical NH₃.

SEM investigations were done on a S510 electron microscope (Scientific Instruments Ltd., Cambridge, U.K.).

Table 1. Selected Technical Details and Results of Rietveld Refinements of Neutron Diffraction Data of Ni₃N Taken at Room Temperature^b

no. of background parameters	12/6/6
no. of profile parameters	4/5/4
min <i>d</i> spacing used for refinement, Å	1.40/0.65/0.50
cell parameters, Å	
<i>a</i>	4.6224 ^a
<i>c</i>	4.3059
positional parameter of Ni, <i>x</i> _{Ni}	0.3279(1)
occupancy ρ (2b)	0.029(2)
100 <i>u</i> (Ni), Å ²	0.517(4)
100 <i>u</i> (N), Å ²	0.476(7)
distances, ^a Å	
<i>d</i> (Ni–Ni)	2 × 2.625, 4 × 2.633, 2 × 2.677, 4 × 2.691
<i>d</i> (Ni–N(2c))	6 × 1.890
cell parameter, Å	
<i>a</i> (NiO)	4.1826
<i>a</i> (Ni)	3.5229
wR _p	1.9/1.7/1.4
R _{Bragg} (Ni ₃ N, <i>F</i> ²), 1σ	2.9/3.2/3.7

^a Standard deviations resulting from Rietveld refinements are not reported here. They are insignificantly small (<0.0001 Å for lattice parameters, <0.001 Å for distances), which is frequently observed.³⁵

^b Structural model: *P*6₃22 (No. 182), *Z* = 2; Ni on 6g, *x*_{Ni}, 0, 0; N on 2c, 1/3, 2/3, 1/4, occupancy 1 – ρ (2b); N on 2b, 0, 0, 0; vacancy on 2d, 2/3, 1/3, 1/4. Data on different detector banks are given for 2θ = 35, 90, and 145°, respectively.

High-Temperature Neutron Diffraction. For neutron diffraction experiments, we combined several batches of Ni₃N. The final sample was 3.3 g of Ni₃N containing small amounts of impurities of NiO and Ni. The powder was placed into a vanadium cylinder of *r* = 4 mm and *h* = 40 mm.

Thermal decomposition of Ni₃N under evolution of N₂ is irreversible and kinetically controlled¹ and proceeds faster in a vacuum than under N₂.²⁰ High N₂ pressures are to be expected in a closed cylinder, which may lead to its destruction. Therefore, we only loosely closed the container with a gold wire as a closure ring. This was done in such a way that the ring was the weakest point in the system, and N₂ pressure is released upon growing too high. This ensures that the sample is not in a vacuum at the beginning of the measurements.

Neutron diffraction experiments were performed at the time-of-flight diffractometer POLARIS installed at the pulsed spallation source ISIS in the Rutherford Appleton Laboratory. Diffraction data were recorded independently on three different detector banks located at about 2θ = 35, 90, and 135° covering different ranges of *d* spacings. Increased sample temperatures were generated by a furnace constructed with a vanadium shield and a continuously evacuated sample chamber. A manometer was used to monitor possible evolution of N₂ from decomposition of the sample. Each temperature step of *T* ≥ 373 K took about 1 h, including change in temperature and for reaching thermal equilibrium.

Rietveld Refinement. For Rietveld refinement, the GSAS package of programs²¹ was used. These programs allow a simultaneous evaluation of the data recorded on the different detector banks.

The nuclear scattering lengths used were *b*(Ni) = 1.03 × 10^{–12} cm, *b*(N) = 0.936 × 10^{–12} cm, and *b*(O) = 0.5805 × 10^{–12} cm.²² The background was fitted by a shifted Chebishev function for each multidetector bank. The reflection profiles were refined using an exponential pseudo-Voigt convolution as implemented in GSAS.

Absorption due to the sample and its environment was refined by a model for linear absorption. The coefficients for each bank were

(13) Juza, R.; Hahn, H. *Z. Anorg. Allg. Chem.* **1938**, 239, 282.

(14) Juza, R.; Rabenau, A. *Z. Anorg. Allg. Chem.* **1956**, 285, 212.

(15) Leineweber, A.; Jacobs, H.; Hüning, F.; Lueken, H.; Schilder, H.; Kockelmann, W. *J. Alloys Compd.* **1999**, 288, 79.

(16) Sørensen, S. P. *Z. Anorg. Allg. Chem.* **1894**, 5, 354.

(17) Kistrup, H. Ph.D. Thesis, RWTH Aachen, Aachen, Germany, 1976.

(18) Jacobs, H.; Schmidt, D. *Curr. Top. Mater. Sci.* **1982**, 8, 379.

(19) Brokamp, Th. Ph.D. Thesis, Universität Dortmund, Dortmund, Germany, 1991.

(20) Bernier, R. *Ann. Chim.* **1951**, 6, 104.

(21) Larson, A. C.; von Dreele, R. B. *GSAS—General Structure Analysis System, Manual*; Los Alamos National Laboratory: Los Alamos, NM, 1994.

(22) Sears, V. F. Chalk River Nuclear Lab.—Internal Report AECL-8490, 1984.

Table 2. Results of Rietveld Refinements of High-Temperature Neutron Diffraction Data Taken of Ni₃N (Further Technical Details Are Those Given for Data Taken at Ambient Temperatures (Table 2))

<i>T</i> , K	<i>a</i> , ^a Å	<i>c</i> , ^a Å	ρ (2b)	x_{Ni}	100 <i>u</i> (Ni), Å ²	100 <i>u</i> (N), Å ²	content of NiO ^b	content of Ni ^b	<i>R</i> _{Bragg} (Ni ₃ N)
298	4.6224	4.3059	0.029(2)	0.3279(1)	0.517(4)	0.476(7)	0.0132(3)	0.0266(4)	3.7/2.9/3.2
373	4.6264	4.3100	0.029(2)	0.3281(1)	0.658(5)	0.558(8)	0.0137(3)	0.0264(4)	2.8/3.2/4.1
423	4.6290	4.3126	0.029(2)	0.3282(1)	0.753(6)	0.629(8)	0.0148(3)	0.0259(4)	3.0/3.6/4.5
473	4.6317	4.3154	0.028(2)	0.3284(1)	0.859(6)	0.704(9)	0.0157(3)	0.0259(4)	3.9/3.8/4.8
498	4.6329	4.3171	0.023(2)	0.3286(2)	0.930(6)	0.777(9)	0.0187(3)	0.0254(5)	4.7/4.2/5.4
523	4.6339	4.3187	0.017(2)	0.3290(2)	0.984(7)	0.82(1)	0.0226(3)	0.0262(5)	5.7/3.8/5.8
548	4.6348	4.3202	0.011(2)	0.3292(2)	1.041(7)	0.86(1)	0.0251(3)	0.0419(6)	6.2/4.8/4.6
573	4.6363	4.3217	0.015(2)	0.3295(2)	1.082(9)	0.89(1)	0.0278(4)	0.199(1)	6.9/4.4/5.8
598	4.6380	4.3230	0.021(4)	0.3294(4)	1.12(2)	0.89(2)	0.0331(5)	0.460(2)	8.2/4.9/7.0

^a Standard deviations resulting from Rietveld refinements are not reported here. They are insignificantly small (<0.0001 Å), which is frequently observed.³⁶ ^b Content referring to the number of Ni atoms.

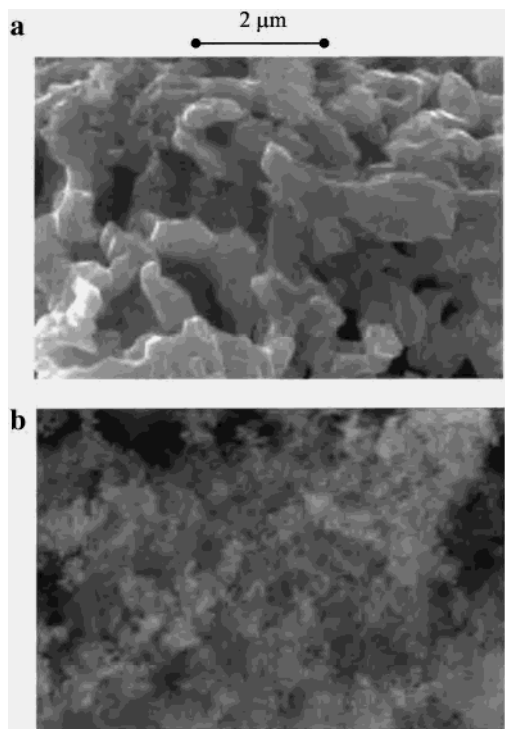


Figure 2. SEM photographs of Ni₃N (magnification = 16000×, black line corresponds to 2 μm): (a) material synthesized in supercritical NH₃ ($p(\text{NH}_3) \approx 2$ kbar) and (b) material from the direct reaction of Ni(NH₃)₆Cl₂ with NaNH₂. Each of the materials was produced at 250 °C.

determined from a simultaneous refinement of data taken at ambient temperatures and 548 K. The obtained coefficients were used as fixed values for all other measuring temperatures.

The nuclear structure used for refinement is based on the ϵ -Fe₃N ideal structure with fixed composition Ni₃N and with allowance for partial disorder of N using a second octahedral site (top of Table 2). Further on, this is called a “disorder” site. It assumes a disorder similar to that found for ϵ -Fe₃N at elevated temperatures.

The presence of NiO and Ni impurities in the sample of Ni₃N was considered by multiphase refinements. Thermal displacement parameters of Ni and O were fixed to those of Ni and N of the Ni₃N phase, respectively, except for the measurements taken at 573 and 598 K. For these, the metallic Ni phase was present in larger amounts and a separate thermal displacement parameter was considered. Furthermore, for all phases, we used one set of profile parameters for each pattern from a particular detector bank.

Results

SEM. Figure 2 shows SEM images of Ni₃N synthesized (a) in supercritical ammonia and (b) by direct solid-state reaction of powdered Ni(NH₃)₆Cl₂ with NaNH₂. Clearly, the first material

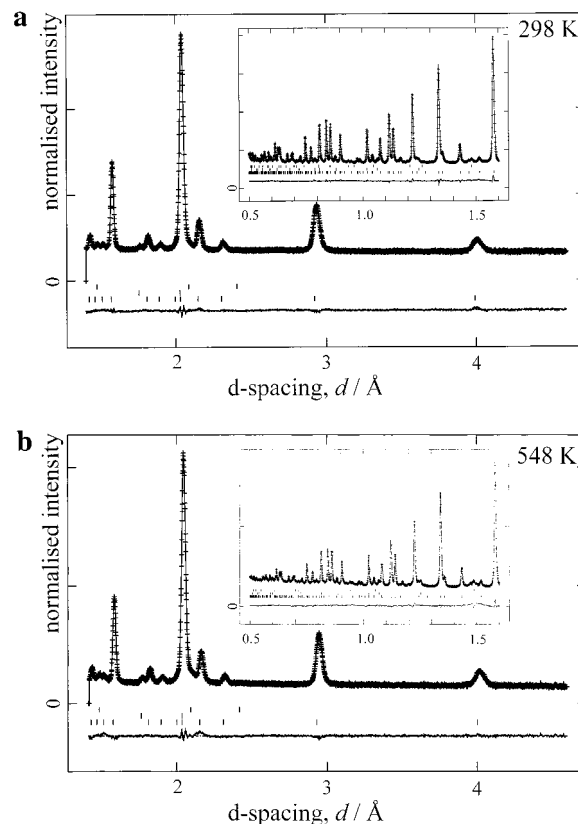


Figure 3. Neutron powder diffraction patterns of Ni₃N (POLARIS (ISIS), detector bank at $2\theta = 35^\circ$): (a) ambient temperatures and (b) 548 K. The insets show the $0.5 \text{ \AA} < d < 1.6 \text{ \AA}$ range of the backscattering bank ($2\theta = 135^\circ$). Reflection markers: NiO, Ni, and Ni₃N (from the top).

is more compact. Transport phenomena within the NH₃ solvent may be responsible for the increased particle size, although attempts to grow single crystals of Ni₃N from NH₃ using various mineralizers including amides have not been successful.⁴

In contrast, the solid-state reaction is difficult to control. Solid NaNH₂ seems to act partially as a reductant to Ni²⁺, before the amide is formed. Ni₃N, once formed, should not decompose to Ni at the reaction temperatures.

Crystal Structure. The high-temperature neutron diffraction experiments were started with a measurement taken at ambient temperatures (Figure 3). Rietveld refinement indicates that the crystal structure is virtually ideal with respect to the distribution of N. The occupied octahedral sites correspond to the position of N in the ϵ -Fe₃N ideal structure. Only about 3% of the N atoms are found on the disorder site 2b (Table 2). The impurities of Ni and NiO are less than 5% (referring to Ni atoms) of the sample.

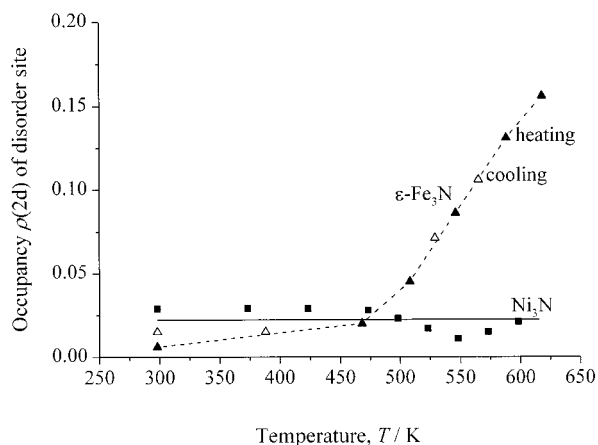


Figure 4. Occupancy of N on the disorder site 2b in $P6_322$ as a function of temperature for Ni_3N and $\epsilon\text{-Fe}_3N$.¹⁵ Lines are not fitted and only give the trend.

As the sample temperature is increased stepwise, the diffraction patterns visually show no changes up to 548 K (Figure 3). Starting from 573 K, the intensity of the reflections for the metallic Ni phase becomes stronger with increasing temperatures. This is accompanied by an increase in pressure in the dynamically evacuated sample chamber. Obviously, Ni_3N decomposes under formation of Ni and N_2 . Up to the maximum sample temperature of 598 K, the Ni content increases strongly whereas the NiO content remains unchanged (Table 2). The reported phase contents are, however, only averages during the data collection period. Cubic Ni_4N ^{20,23} was not observed as an intermediate phase.

Rietveld refinement (Table 2) of the high-temperature diffraction data does not show significant changes in the distribution of N with increasing temperatures. These results have to be compared with what has been observed for $\epsilon\text{-Fe}_3N$.¹⁵ In Figure 4, the occupancy of the disorder site 2b by N is plotted for $\epsilon\text{-Fe}_3N$ and Ni_3N . In contrast to Ni_3N , significant disorder is found for $\epsilon\text{-Fe}_3N$ with a maximum measuring temperature of about 600 K. For $\epsilon\text{-Fe}_3N$, the significant disorder is readily detected from visual inspection of the diffraction patterns.

Order-disorder phenomena in interstitial compounds can be regarded as being driven by configurational entropy, which, at increased temperatures, may overcome a state of lowest enthalpy leading to disorder.²⁴ The comparison of the data of the isotopic compounds obviously indicates that repulsive interactions between the N atoms, the reason for the ordered occupation of one-third of the octahedral sites, may be higher in Ni_3N than in isotopic $\epsilon\text{-Fe}_3N$.

A physical reason for this may be the shorter interatomic distances of $N\cdots N$ in Ni_3N compared to those in $\epsilon\text{-Fe}_3N$: moving with increasing atomic numbers of the metals from Fe_3N to Ni_3N , one observes a considerable contraction of the unit cell parameters (from 4.694 to 4.622 Å for a , and from 4.375 to 4.306 Å for c). In the simplest models, the interactions of $N\cdots N$ (like some kind of Coulomb repulsion between ions, but the main mechanisms governing the pair interactions for N in interstitial compounds are probably the so-called strain-induced interactions)^{24,25} should increase as their distances are reduced with decreasing unit cell parameters. Therefore, the disordering of N should be more difficult for Ni_3N than for $\epsilon\text{-Fe}_3N$.

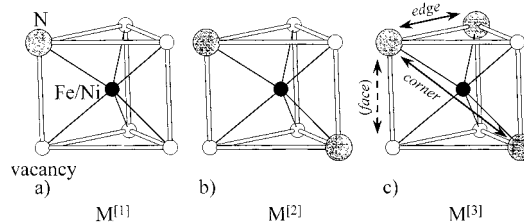


Figure 5. (a–c) Coordination spheres $M^{[1]}$, $M^{[2]}$, and $M^{[3]}$ relevant for the discussion of the disordering of N in $\epsilon\text{-Fe}_3N$ and Ni_3N . The first three closest possible distances of $N\cdots N$ are depicted, which correspond to NM_6 octahedra sharing common corners (distance in Ni_3N at ambient temperatures: 3.43 Å), edges (2.67 Å) and faces (2.15 Å). Face sharing does not occur for the three coordination spheres shown here.

This can be examined more closely on a local scale. In an *hcp* arrangement of M, each M is “coordinated” by six octahedral sites forming a trigonal prism. In the $\epsilon\text{-Fe}_3N$ -type structure, two of these sites are occupied by N. This is illustrated in Figure 5b and shows that NM_6 octahedra share only corners. This coordination will be called $M^{[2]}$ as suggested to assign coordination numbers.²⁶

Statistical considerations show that the occupation of site 2b, as occurring in $\epsilon\text{-Fe}_3N$ at elevated temperatures, leads to a partial formation of the environments $Fe^{[1]}$ and $Fe^{[3]}$ depicted as $M^{[1]}$ (Figure 5a) and $M^{[3]}$ (Figure 5c), respectively. Mössbauer spectroscopy is able to detect separate signals for the different environments and shows that only $Fe^{[2]}$ is present for slowly cooled $\epsilon\text{-Fe}_3N$; $Fe^{[1]}$ and $Fe^{[3]}$ are additionally observed for samples quenched from elevated temperatures.²⁷ The environment $Fe^{[3]}$ is accompanied by the presence of octahedra NM_6 sharing common edges. The disordering can then be described on a local scale as a “disproportionation” $2Fe^{[2]} \rightleftharpoons Fe^{[1]} + Fe^{[3]}$. Furthermore, $Fe^{[3]}$ is also needed to achieve N contents higher than that of Fe_3N , i.e., $\epsilon\text{-Fe}_3N_{1+x}$ ($x \leq 0.48$).^{8,28} $\zeta\text{-Fe}_2N$ ^{29,30} contains only $Fe^{[3]}$.

Ni_3N , however, has no significant range of homogeneity (Ni_3N_{1+x} is restricted to $x = 0$). This is in contrast to other hexagonal interstitial compounds with “ ϵ -type” structure,⁵ including the ϵ -type nitrides of the metals Fe and Co,^{31,32} followed by Ni in the periodic table. This means that in Ni_3N , both processes which would generate $Ni^{[3]}$ (N contents higher in composition than Ni_3N and disordering of N in Ni_3N) are somehow suppressed. The formation of an environment $Ni^{[3]}$ can only be achieved by NNi_6 octahedra sharing common edges. This seems to be unfavored for nickel, e.g., because of the geometric reasons as given above.

For simplicity, we discussed here the ordering of N in terms of deviations from the $\epsilon\text{-Fe}_3N$ ideal structure and not in terms of order parameters. The latter has been done previously^{11,28,33} for different ϵ -type nitrides of 3d metals using concepts and formalisms^{10,11} and will be done in full together with data from structurally similar manganese nitrides.³⁴

(23) Terao, N.; Berghezan, A. *J. Phys. Soc. Jpn.* **1959**, *14*, 139.

(24) de Fontaine, D. *Solid State Phys.* **1979**, *34*, 73.

(25) Hillert, M.; Jarl, M. *Acta Metallurg.* **1977**, *25*, 1.

(26) Lima-de-Faria, J.; Hellner, E.; Liebau, F.; Makovichky, E.; Parthé, E. *Acta Crystallogr., Sect. A* **1990**, *46*, 1.

(27) Eickel, K. H.; Pitsch, W. *Phys. Status Solidi.* **1970**, *39*, 121.

(28) Leineweber, A.; Jacobs, H.; Hüning, F.; Lueken, H.; Kockelmann, W. *J. Alloys Compd.* **2001**, *316*, 21.

(29) Jack, K. H. *Proc. R. Soc. London, Ser. A* **1948**, *195*, 34.

(30) Rechenbach, D.; Jacobs, H. *J. Alloys Compd.* **1996**, *235*, 34.

(31) Juza, R.; Sachsze, W. *Z. Anorg. Allg. Chem.* **1945**, *253*, 95.

(32) Clarke, J.; Jack, K. H. *Chem. Ind. (London)* **1951**, 1004.

(33) Leineweber, A.; Jacobs, H.; Kockelmann, W.; Hull, S. *Physica B* **2000**, *276–278*, 266.

(34) Leineweber, A.; Jacobs, H.; Kockelmann, W.; Hull, S. To be published.

Finally, it should be pointed out that the higher stability of ordering in Ni₃N compared to that in ϵ -Fe₃N seems to be in contrast to its lower stability toward thermal decomposition under loss of N₂. ϵ -Fe₃N_{1+x} starts to decompose at about 670–770 K,³⁵ whereas Ni₃N begins at 570 K as observed here. This shows that the ordering energy is only a small part of the overall energy of formation of these nitrides.

(35) Goodeve, C. F.; Jack, K. H. *Discuss. Faraday Soc.* **1948**, *4*, 82.

(36) Young, R. A. *The Rietveld Method*; Oxford University Press: New York, 1993.

Acknowledgment. Financial support by the “Bundesministerium für Bildung, Wissenschaft, Forschung und Technologie” (JA5DOR), by the “Deutsche Forschungsgemeinschaft”, and by the “Fonds der Chemischen Industrie” is gratefully acknowledged.

Supporting Information Available: X-ray crystallographic file in CIF-format for the Rietveld refinement of the high-temperature neutron diffraction data on Ni₃N. This material is available free of charge via the Internet at <http://pubs.acs.org>.

IC0104860